Available online at www.sciencedirect.com
SCIENCE DIRECT
Polymer 47 (2006) 2884–2893
polymer
www.elsevier.com/locate/polymer

In situ WAXD study of structure changes during uniaxial deformation of ethylene-based semicrystalline ethylene–propylene copolymer

Li-Zhi Liu [a,1], Benjamin S. Hsiao [a,*], Shaofeng Ran [a,2], Bruce X. Fu [a,3], Shigeyuki Toki [a], Feng Zuo [a], Andy H. Tsou [b], Benjamin Chu [a]

[a] *Department of Chemistry, Stony Brook University, Stony Brook, NY 11794-3400, USA*
[b] *Butyl Polymer Technology, ExxonMobil Chemical Company, Baytown, TX 77522, USA*

Received 12 December 2005; received in revised form 26 January 2006; accepted 27 January 2006
Available online 3 March 2006

Abstract

In situ strain-induced structure changes during uniaxial deformation of an ethylene–propylene copolymer, containing 78 wt% (or 85 mol%) of ethylene moiety, were studied by synchrotron wide-angle X-ray diffraction (WAXD). The chosen sample could crystallize into orthorhombic, pseudo hexagonal or a mixed form, depending on the annealing conditions. Crystallization at high temperatures (e.g. 50 °C) favored the formation of orthorhombic form, while crystallization at low temperatures (e.g. 20 °C) favored the formation of pseudo hexagonal form. Under deformation, the transition from orthorhombic to pseudo hexagonal form was observed at relatively low strains (e.g. 0.12). At higher strains, WAXD data indicated the occurrence of direction-dependent crystal destruction at strains <0.25 and subsequent re-crystallization with extended-chain conformation at high strains (>1.0) all of the pseudo hexagonal form. The drastic changes in the crystalline structures (orthorhombic to pseudo hexagonal) and phase transitions (crystal destruction and re-crystallization) at modest strains can be attributed to the high mobility of the amorphous ethylene–propylene segments at room temperature.

Keywords: Ethylene–propylene copolymer; Deformation; X-ray diffraction

1. Introduction

Ethylene–propylene (EP) copolymers have become an important class of thermoplastic elastomers, exhibiting some excellent physical properties. A wide range of properties can be obtained in these materials by the control of copolymer composition [1]. For example, two different classes of EP elastomers are available commercially: ethylene-based copolymer with ethylene being the major component and propylene-based copolymer with propylene being the major component. As ethylene crystals are formed in the ethylene-based EP copolymer and propylene crystals are formed in the propylene-based crystals, their properties are closely associated with the characteristics of the constituting crystals, such as melting point and their corresponding structure changes upon deformation.

In this study, we are mainly concerned with the behavior of an ethylene-based EP copolymer having 78 wt% (or 85 mol%) of ethylene moiety. In ethylene-based EP copolymers, the lower the ethylene content (or the higher the propylene content), the lower the crystallinity as well as the corresponding melting point. In fact, the EP copolymers with ethylene content lower than 60 wt% are essentially amorphous [2]. The significant change in the melting point with decreasing ethylene content (or increasing propylene content) is caused by the reduction of the crystal size from the ethylene sequence, whereas the corresponding structural behavior during static and dynamic conditions can also be altered. For example, a recent study by de Ballesteros et al. [3] indicated that the insertion of the propylene moiety in the lattice of orthorhombic crystal structure from the ethylene sequence gradually increased the disorder in the crystalline phase and eventually led to a pseudo hexagonal crystalline structure at high-propylene content.

There have been several studies on the relationships among structure, morphology and properties for ethylene-based EP

* Corresponding author. Tel.: +1 631 632 7793; fax: +1 631 632 6518.
E-mail address: bhsiao@notes.cc.sunysb.edu (B.S. Hsiao).
[1] Present address: The Dow Chemical Company, 2301 Brazosport Blvd. B-1470, Freeport, TX 77541, USA.
[2] Present address: Symyx Technologies, Inc., 3100 Central Expressway, Santa Clara, CA 95051, USA.
[3] Present address: Hybrid Plastics, Inc., 118 College Dr. #10003, Hattiesburg, MS 39406, USA.

0032-3861/$ - see front matter © 2006 Elsevier Ltd. All rights reserved.
doi:10.1016/j.polymer.2006.01.090

copolymers [4–6]. For example, the crystallization study of copolymers based on ethylene with α olefins by Hiltner, Baer and coworkers [7] suggested that the crystalline morphology could be categorized into two types, when the density is below 0.91 g/cm^3: (1) the observation of fringed-micellar crystalline morphology without the presence of spherulites (density less than 0.89 g/cm^3), and (2) the coexistence of both fringed-micellar and lamellar crystalline morphologies in the presence of spherulites (density between 0.89 and 0.91 g/cm^3). However, in situ structure and morphology studies during deformation are still relatively rare. Understanding of the crystalline structure development in the EP copolymer at molecular and lamellar levels in real time under deformation, and its impact on the elastic properties is essential for many practical applications. Time-resolved synchrotron small-angle X-ray scattering (SAXS) and wide-angle X-ray diffraction (WAXD) techniques are ideally suited for this purpose. These techniques have been used routinely in recent years to obtain dynamic structural and morphological information during polymer processing in solids as well as in melts, such as stretching, spinning and shearing [8–11].

In our previous paper [12], the synchrotron SAXS technique was used to study the lamellar structure changes in ethylene-based semi-crystalline ethylene–propylene copolymers. Results indicated that, above the strain of 0.74, strain-induced crystallization, possibly with extended-chain conformation, began to occur. The newly developed crystals coexisted with re-oriented original crystals, forming an effective crystalline scaffold that significantly enhanced the mechanical properties. It appeared that the original crystals melted away completely at a strain of 1.5, and the fraction of strain-induced crystals increased continuously with strain. When the elastomer was stretched to a strain of 1.9 and then relaxed to zero load, most strain-induced crystals surprisingly remained aligned along the stretching direction. The evidence of crystal destruction (or mechanically-induced melting) and re-crystallization processes during deformation, however, was somewhat indirect by the SAXS study, which motivated us to carry out the in situ WAXD study of the same EP copolymer under the same deformation conditions in this work. WAXD results provided clear evidence of strain-induced crystal destruction and subsequent re-crystallization processes. In addition, the structure changes, resulting from variations in crystallization and deformation conditions, were obtained. By combining our previous SAXS results [12] and WAXD data in this study, a thorough understanding of the structure changes in the ethylene-based semicrystalline EP copolymer during deformation was obtained at both lamellar and molecular levels.

2. Experimental

The material studied in this work was the commercial Vistalon V805 ethylene–propylene (EP) elastomer from ExxonMobil Chemical Company. The material is a typical EP copolymer, prepared by a conventional vanadium catalyst. This polymer contained 78 wt% or 85 mol% of ethylene moiety having the number-average molecular weight $M_n = 7.6 \times 10^4$ g/mol and the weight-average molecular weight $M_w = 1.7 \times 10^5$ g/mol. Since the chosen sample is a random ethylene–propylene copolymer with 22 wt% of propylene moiety, it has much weaker crystallization ability than polyethylene homopolymer. The final crystallinity (ca. 15%) of the copolymer very much depends on the crystallization time and the measurement technique (DSC or X-ray). The crystallinity obtained from the X-ray diffraction method could vary in the cases of crystallization for hours or for days. The sample was melt-pressed at 160 °C into film with a thickness about 1 mm. The pressed films were crystallized under two different conditions. (1) The film was first heated up to 160 °C for 10 min in an oven, quickly taken out and annealed at ambient conditions for 1 week before measurement. (2) The film was first heated up to 160 °C for 10 min in an oven, quickly placed into another oven with a preset temperature at 50 °C for 2 h, then taken out and annealed at ambient conditions for 48 h before measurement. The samples prepared with methods (1) and (2) were used for static X-ray measurements to determine the crystal structure. The sample prepared with method (2) was also used for in situ deformation study. Static WAXD measurements were further carried out on samples prepared by methods (3) and (4) in a dual-chamber temperature jump apparatus to correlate with the DSC study: (3) the sample was melted at 160 °C for 10 min and then rapidly cooled to 20 °C for isothermal crystallization of 48 h; (4) the sample was melted at 160 °C for 10 min and then rapidly cooled to 50 °C for isothermal crystallization of 48 h. Time-resolved WAXD measurements were also carried out in a Linkam hot stage to follow the non-isothermal crystallization process using the following two protocols: (5) the sample was cooled from 160 °C to room temperature at 10 °C/min, (6) the sample was cooled from 160 °C to room temperature at about 30 °C/min, as a referenced study.

Both static and in situ WAXD experiments together with mechanical measurements were performed at the Advanced Polymer Beamline (X27C) in the National Synchrotron Light Source (NSLS), Brookhaven National Laboratory (BNL). The wavelength used was 0.1366 nm. The WAXD profiles shown in this study were converted to the wavelength of 0.1542 nm, in order to be compared with the literature results. A two-dimensional (2D) MAR CCD X-ray detector was used for real-time data collection during deformation. The diffraction angle was calibrated with an Al_2O_3 standard. The deformation experiment was carried out in a modified Instron 4442 tensile apparatus [13]. A symmetrical stretching mode was used, where the detection spot by synchrotron beam on the sample remained fixed in space. Rectangular samples with dimensions of 60 mm × 10 mm × 1 mm were used for the deformation experiment. The sample length between the Instron clamps was 30 mm. The experiments were carried out at room temperature (25 °C). A constant extension rate (10 mm/min) was applied to the specimen throughout the deformation process. No necking was observed. WAXD images were taken immediately after the desired strain was reached during either the stretching or relaxation process. The data collection time for each image was 25 s. Background scattering and beam intensity fluctuations

were corrected on the measured pattern. The missing diffraction intensity along the stretching direction (i.e. the meridional direction, assuming the deformed sample has a fiber symmetry) collected from the flat CCD camera was also estimated by using the Fraser method with Legendre expansion [13].

3. Results and discussions

It is well known that the crystalline structure in ethylene-based EP copolymer containing high-ethylene content usually exhibits an orthorhombic unit cell with typical dimensions of $a=7.4$ Å, $b=4.93$ Å, $c=2.54$ Å [3]. While the orthorhombic crystal structure is the most stable form in polyethylene homopolymer, a transition from orthorhombic to pseudo hexagonal form has also been reported under some circumstances, e.g. ultrahigh molecular weight polyethylene (UHMWPE) under extensional deformation at high temperatures near its melting point [14,15]. For the EP copolymer studied in this work, it exhibited much weaker crystallization ability than conventional polyethylene homopolymer. For example, non-isothermal scans by differential scanning calorimetry (DSC) (Fig. 1) showed that crystallization and subsequent melting responses of this system are very different from those of typical polyethylene, due to the random insertion of methyl branches along the ethylene chains. During the cooling process (e.g. at −10 °C/min from 100 to −40 °C), the crystallization temperature of an EP copolymer is around 40 °C, significantly lower than that of typical polyethylene (ca. 110 °C). The curves shown in Fig. 1 are part of the whole cooling and melting curves in the range of 4–96 °C; the truncation allows the identification of main thermal features during cooling and melting processes. In addition, the crystalline peak covers a very broad range, from 0 to 60 °C, which is due to the broad sequence distribution of ethylene moiety in the chains—crystals arising from short ethylene sequences melt at lower temperatures. A very broad melting peak was also seen during the subsequent heating process with the peak temperature at about 54 °C. The broad melting peak is basically due to the formation of crystals with a large range of size, again resulted from the broad sequence distribution of ethylene moiety. Besides the effect of crystal size, the different crystal form and morphology may also contribute to the broad range of the melting peak. For the copolymer in this study, the majority of crystals probably possess a fringe-micelle like structure (from short ethylene sequences) in conjunction with a small amount of lamellar stacks (from long ethylene sequences). The former would exhibit a lower melting point and the latter would have significantly higher melting point. From the structure point of view, as mixed pseudo hexagonal and orthorhombic structures could co-exist, the pseudo hexagonal structure should contribute more to the lower melting point and the orthorhombic structure should contribute more to the higher melting point.

It has been reported that in the EP copolymer with ethylene content of 89.4 mol%, only an orthorhombic crystal form was seen [15]. Hu et al. [16] showed that the crystalline structure changed from orthorhombic to pseudo hexagonal form by decreasing the ethylene content to 80.1 mol%. The study by de Ballesteros et al. [3] also demonstrated that the pseudo hexagonal structure formed in a stretched EP copolymer with 75 mol% of ethylene content. In the present study, our results indicated that in EP copolymer with 85 mol% ethylene content, made by vanadium catalyst, both orthorhombic and pseudo hexagonal forms could be produced, depending on the crystallization conditions. In addition, the transition from orthorhombic to pseudo hexagonal form could be induced by tensile deformation. These results are described as follows.

3.1. Different crystalline structures obtained at varying crystallization conditions

Prior to the deformation study, static WAXD measurements were carried out on samples prepared under different crystallization conditions. The first sample was prepared by thermal treatment (1) in the experimental section, i.e. the sample was melted at 160 °C for 10 min, quenched to room temperature (at about 20 °C) and then crystallized for 1 week. The WAXD intensity profile of such a crystallized EP copolymer sample is shown in Fig. 2. Only one strong diffraction peak was seen at 20.7° (at the wavelength of 0.1542 nm), which was very

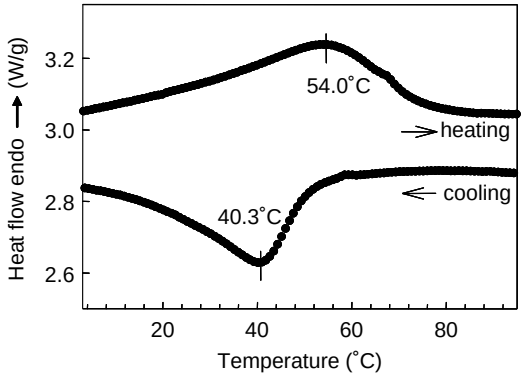

Fig. 1. DSC thermograms during cooling from 100 to 0 °C at a rate of 10 °C/min; the subsequent heating was carried out at the same rate.

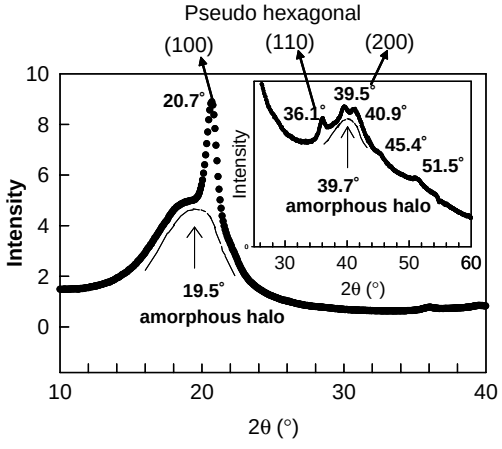

Fig. 2. Linear WAXD profile of the EP copolymer annealed at 160 °C for 10 min and then quenched to room temperature to crystallize for several days.

different from the typical diffraction profile in polyethylene with two strong diffraction peaks between 20 and 25°, i.e. (110) and (200) reflections from the orthorhombic form. Several weak but distinct diffraction peaks were also seen at around 40° (shown in the inset of Fig. 2), indicating that the sample possessed a pseudo hexagonal form [3] (the corresponding three major reflections: (100), (110) and (200) were indexed in Fig. 2). We also carried out time-resolved WAXD measurements of a molten sample cooled from 160 °C to room temperature at two different cooling rates: 10 and 30 °C/min (thermal treatments (5) and (6) as described in the experimental section), using a Linkam hot stage. No diffraction peak (i.e. no WAXD crystallinity) was seen during either cooling scan or after the samples were held at room temperature for a couple of hours. This observation was consistent with the results from a study by Mathot et al. [6], who have conducted a time-resolved simultaneous SAXS–WAXS–DSC study of ethylene–octene random copolymer with 87 mol% of ethylene content. They showed that crystal reflections in WAXD appeared at much lower temperatures than the crystallization temperature in DSC. This suggests that although the exothermic peak (at about 40 °C) observed in the cooling scan of DSC (Fig. 1) is associated with the occurrence of crystallization, it does not necessarily represent the completion of three-dimensional ordered packing, which would take a much longer time to develope at lower temperatures. It is conceivable that the high crystallographic ordering of the pseudo hexagonal crystalline structure is mainly due to the annealing process at room temperature. We hypothesize that the exothermic peak in DSC cooling scan may be partially due to the segregation of ethylene sequences, which would lead to an increase of local ordering without forming crystals with ordered three-dimensional structures. Such a process can release a great deal of latent heat, but the resulting structure cannot be clearly detected by WAXD.

WAXD profiles of the sample annealed at 50 °C with thermal treatment (4) (i.e. the sample was melted at 160 °C for 10 min, quenched to 50 °C and isothermally crystallized for 48 h) and of the sample annealed at 20 °C with thermal treatment (3) (i.e. the sample was melted at 160 °C for 10 min, quenched to 20 °C and isothermally crystallized for 48 h) are shown in Fig. 3. It is interesting to note that the profile from the sample crystallized at 50 °C exhibited two crystal diffraction peaks—a strong diffraction peak at 20.7° and a weak diffraction peak at 22.3°, which could be indexed as (110) and (200) reflections, respectively, from the orthorhombic form. The sample annealed at 20 °C for 48 h still exhibited the dominant pseudo hexagonal form. We note that the peak at 20.7° cannot be solely assigned to the orthorhombic structure. This is because the intensity of the peak at 20.7° is too strong compared to that at 22.3° (i.e. the (200) reflection of the orthorhombic structure) as seen in Fig. 3. In addition, the (110) reflection from the typical orthorhombic form is located at a slightly higher angle (21.3°) than the observed one (20.7°) when the copper radiation is used. Thus, it is more likely that the peak at 20.7° consists of both crystalline structures. From the above observations, we conclude that different crystalline forms can be obtained under varying crystallization conditions in the chosen EP copolymer. At high-annealing temperatures (e.g. 50 °C), the crystallization process of the ethylene sequences is slower, but it enables the formation of larger crystals with a more stable orthorhombic form. At low annealing temperatures (e.g. room temperature), the crystallization process is faster. However, the process favors the formation of small crystals with the metastable pseudo hexagonal form. It is imperative to point out that DSC and X-ray experiments examine different aspects of the crystallization behavior. During the cooling process, no diffraction signal was observed by WAXD, which was consistent with the literature data [6]. However, the DSC cooling thermogram showed a broad exothermic peak and corresponding SAXS patterns also detected a distinct two-phase structure [12]. The absence of X-ray diffraction does not mean that no structure formation takes place during cooling, it simply means that the formed structures do not possess distinct three-dimensional ordering or they are too small to be detected (e.g. small crystallites) by WAXD.

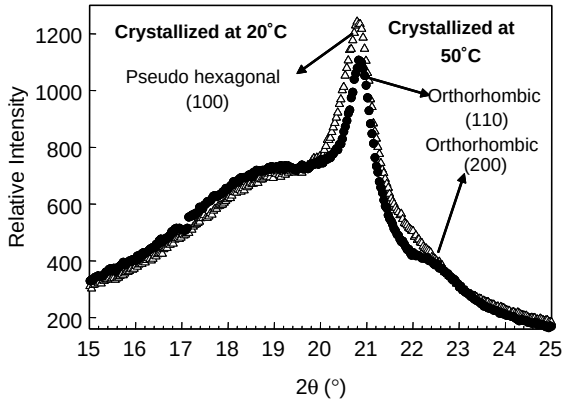

Fig. 3. Linear WAXD profiles of the EP copolymer crystallized at 20 and 50 °C for 48 h, respectively, after the sample was melted at 160 °C for 10 min.

The crystallite size (L) can be estimated from the breadth of the diffraction peak using the Scherrer equation [17]

$$L = \frac{0.94\lambda}{B(2\theta)\cos\theta} \quad (1)$$

where λ, 2θ and $B(2\theta)$ represent the wavelength, the diffraction angle and the width (in radian) at the half maximum intensity. For each hkl-reflection, the value of L can be approximately interpreted as an average crystal dimension perpendicular to the reflecting plane. The crystal size corresponding to the main diffraction peak in both cases was calculated using this equation. The estimated crystal dimension perpendicular to the 100 plane in the pseudo hexagonal form (Fig. 3, sample crystallized at 20 °C or room temperature) was about 14 nm, whereas that of the 110 plane in the orthorhombic form was about 23 nm. The real difference in the crystal size may be much larger than the above estimate, as the peak at 20.7° may partially contain the pseudo hexagonal structure as discussed above.

The crystalline structure for the sample with thermal treatment (2) (i.e. the sample was first heated up to 160 °C

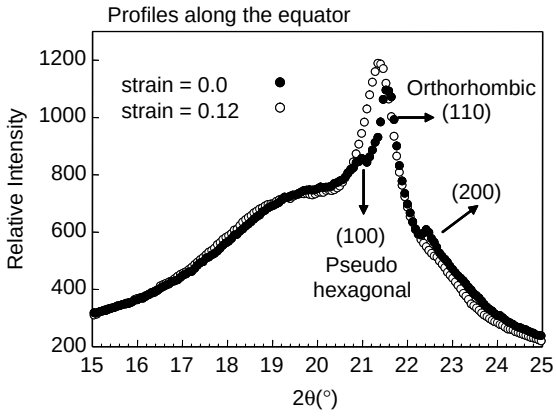

Fig. 4. Linear WAXD profiles at two different strains (0.0 and 0.12), taken along the equator. The EP copolymer was first crystallized at 50 °C for 2 h, and then quenched to room temperature and annealed for 48 h.

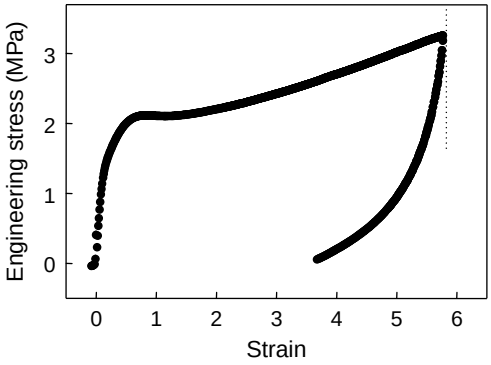

Fig. 5. The stress–strain curve for the extension and retraction processes of the EP copolymer that was first crystallized at 50 °C for 2 h and then quenched to room temperature and annealed for 48 h (the deformation rate was 10 mm/min).

for 10 min, quickly quenched to 50 °C for 2 h and then annealed at ambient conditions for 48 h) was also studied. Fig. 4 shows the WAXD profiles taken along the equatorial direction for this sample at two mechanical conditions: strain = 0 and 0.12 (the profile at strain = 0.12 will be discussed later). The profile at strain = 0 exhibited three distinct diffraction peaks: (110) and (200) reflections from the orthorhombic form at higher diffraction angles and (100) reflection from the pseudo hexagonal form at a lower angle (20.7°). Comparing the coexistence of mixed orthorhombic and pseudo hexagonal forms in the sample with thermal treatment (2) (crystallization at 50 °C for 2 h and subsequently at room temperature for 48 h) with the pure orthorhombic form (Fig. 3) in the sample with thermal treatment (4) (crystallization at 50 °C for 48 h), we came to the following conclusion. Annealed at 50 °C, the orthorhombic form was formed, but the crystallization rate might be very slow. We believe that annealing at 50 °C for a short period of time (2 h) can nucleate the orthorhombic form (even though small in size), and further annealing at a lower temperature (20 °C) can facilitate the growth of both orthorhombic and pseudo hexagonal forms. That is, crystallization at higher temperatures (e.g. 50 °C) favors the formation of orthorhombic form; whereas crystallization at lower temperatures (e.g. 20 °C) favors the formation of pseudo hexagonal form.

3.2. Deformation-induced crystal destruction and crystal structure change at low strains

For the deformation study, the sample crystallized with thermal treatment method (2) was used. The rationale for the selection of this sample is because we were particularly interested in the investigation of the stability in different crystal forms (orthorhombic versus pseudo hexagonal) under deformation. The typical stress–strain curve, during extension and retraction processes, is shown in Fig. 5 (the maximum strain was about 6.0). During the extension process, a yield point at the strain of about 0.75 was seen. It was interesting to note that the majority of structure and morphology changes occurred at low strains, significantly below the yield point.

The equatorial WAXD profile taken at strain = 0.12 is shown in Fig. 4. It was interesting to note that even with such a small strain, deformation could completely eliminate the orthorhombic form. In Fig. 4, the (110) reflection from the orthorhombic form and the (100) reflection from the pseudo hexagonal form in the sample with no strain merged into a single peak (at a diffraction angle between the two reflections) in the sample with strain = 0.12. This indicates that the orthorhombic form changed into the pseudo hexagonal form. Since the deformation was carried out at a relatively small strain (e.g. 0.12) and in a short period of time, we believe that the transformation from orthorhombic to hexagonal structures probably took place by a solid-to-solid phase (mastensitic) transition, instead of passing through the amorphous phase and then re-crystallizing into the hexagonal structure. It was seen that the total diffraction intensity on the equator at strain 0.12 became larger than that before deformation, which could be attributed to the rotation of some crystals along the stretching direction. On the other hand the scattering contributions from the amorphous phase were near identical before and after deformation. It is difficult to determine if there is any peak shifting in the pseudo hexagonal form during deformation, since the diffraction from the pseudo hexagonal form prior to deformation is very small compared with that from the orthorhombic form. The corresponding intensity profiles taken along the stretching direction at different strains are shown in Fig. 6. At the strain of 0.12, the orthorhombic form (the dominant phase) disappeared, leaving behind only the pseudo hexagonal form. It is unlikely that under such a small strain (i.e. 0.12), all the orthorhombic crystals would be oriented perfectly along the stretching direction, such that the diffraction on the meridian could be absent (due to the Ewald sphere) [18]. In other words, the disappearance of the orthorhombic form at such a small strain suggests that some crystals must be destroyed under deformation (it is necessary to point out that the measured diffraction intensity was not corrected for the sample thickness change, but the crystal destruction noticed here is not based on the change in intensity, but the totally disappearance of diffraction peaks from the orthorhombic form). Form above results, we conclude that

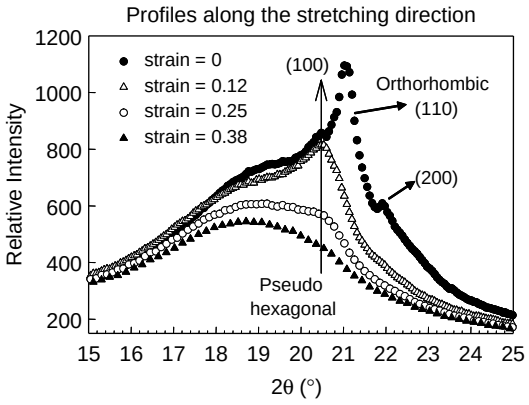

Fig. 6. Linear WAXD profiles at different strains (0.0, 0.12, 0.25 and 0.38) for the same EP copolymer crystallized as that in Fig. 4.

during small deformation of the chosen EP copolymer, the following three events can all occur: (1) crystal destruction (or mechanically-induced 'melting'), (2) stress-induced solid–solid transition (from orthorhombic to hexagonal), and (3) reorientation of crystals along the stretching direction. Furthermore, we hypothesize that the crystals, with their chains already aligned along the stretching direction before deformation, may be more susceptive to undergo the solid-to-solid transition and change the structure from orthorhombic to hexagonal; whereas the crystals, with their chains aligned perpendicular to the stretching direction before deformation, may be more susceptive to be destroyed during deformation. In addition, we suggest that the pseudo hexagonal form is more energetically stable in this copolymer than the orthorhombic form under strained conditions.

In Figs. 4 and 6, it is also seen that the width of the (110) reflection from the orthorhombic form before deformation is much smaller than that of the (100) peak from the hexagonal form after deformation. Using Eq. (1), the estimated crystal sizes corresponding to the initial orthorhombic (110) and the pseudo hexagonal (100) reflections under deformation were 23 and 14 nm, respectively. These results indicated that the crystal size decreased with deformation even at a very low strain (e.g. 0.12). However, the real difference in crystal size could be smaller than the estimated value, since the diffraction peak at strain of 0.12 could also contain some remaining orthorhombic crystals as described above. The behavior of strain-induced crystal destruction at low strains could also be concluded from the following results. Selected three-dimensional (3D) diffraction patterns at different strains are shown in Fig. 7(a). It was seen that at low strains (e.g. 0.12, data not shown), the dominant reflection at 20.7° from the pseudo hexagonal form was split into four arcs around the equator as illustrated in the WAXD profiles at strains of 0.25 and 0.52. The formation of the four-point pattern seen in Fig. 7(a) could be explained by the tilting of the maximum shear force with respect to the uniaxial stretching direction (usually at a 45° angle), where some crystals were destroyed by yielding and residual crystals were aligned with their slip plains parallel to the shear direction. Fig. 7(a) shows that at strain 0.25, the diffraction volume was decreased almost by half (e.g. the intensity at the position of the four-point maxima at strain 0.25 was only slightly higher than that before deformation, but the intensity almost lost all its value along the stretching direction under deformation). Again, we note that the intensity shown in Fig. 7(a) was not corrected for the sample thickness change.

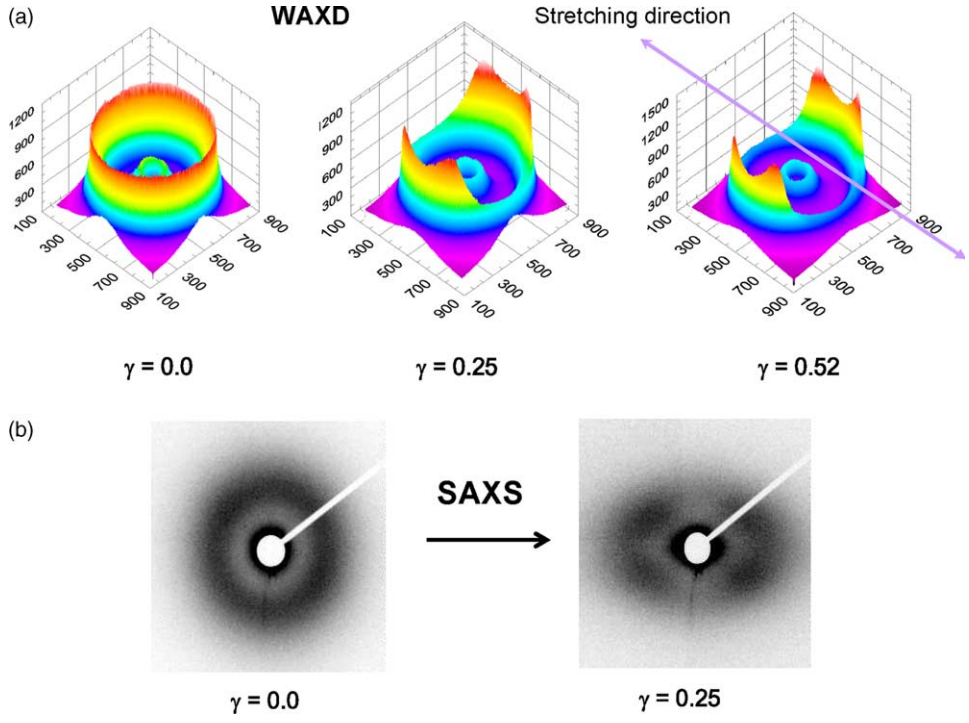

Fig. 7. (a) 3D WAXD profiles of the EP copolymer at strains of 0.0, 0.12 and 0.25; (b) 2D SAXS patterns taken at strains of 0.0 and 0.25.

This result suggests that the pseudo hexagonal crystals can be formed at a small strain (e.g. 0.12), but it also can be destroyed at least partially with increasing strain (e.g. 0.25).

At a higher strain (e.g. 0.38), the shape and position of the (100) reflection from the pseudo hexagonal form along the equator did not show any changes (data not shown), however, this reflection along the stretching direction (or meridional direction) disappeared almost entirely (Fig. 6). If such disappearance was due to the orientation of the pseudo hexagonal form, then the (100) reflection should be shifted to the equator and a large increase in the equatorial intensity would be observed, but it was not seen. This finding suggests that the mass fraction of the pseudo hexagonal form must decrease with increasing strain. In fact, the yield point of the material was found at a strain about 0.75 (Fig. 5), where our earlier SAXS data exhibited a minimum scattering power [12]. These results suggest that the pseudo hexagonal crystals, originally transformed from the orthorhombic form by deformation, are mostly destroyed when the material reaches the yield point and new crystals start to form afterward. The detailed mechanism of the structure changes at the lamellar and molecular levels can be described as follows, based on the combined SAXS and WAXD results.

Fig. 7(b) shows corresponding SAXS patterns collected at the strain of 0.25. It was seen that the total scattered intensity (the invariant) decreased significantly and the scattering pattern became anisotropic with four distinctive arc-like scattering peaks. In our earlier study [12], we argued that this behavior is due to the fragmentation of some crystalline lamellae, particularly those with their long axes aligned perpendicularly to the stretching direction. This is because in these lamellae, some chain segments, aligned parallel to the stretching direction, can be pulled out even at low strains, resulting in the checker-board formation of residual crystallites. This argument still holds here and is consistent with the WAXD results. The fragmented crystals have smaller sizes and their axes tilted with respect to the stretching direction. This morphology, along with that of the re-oriented but unaffected

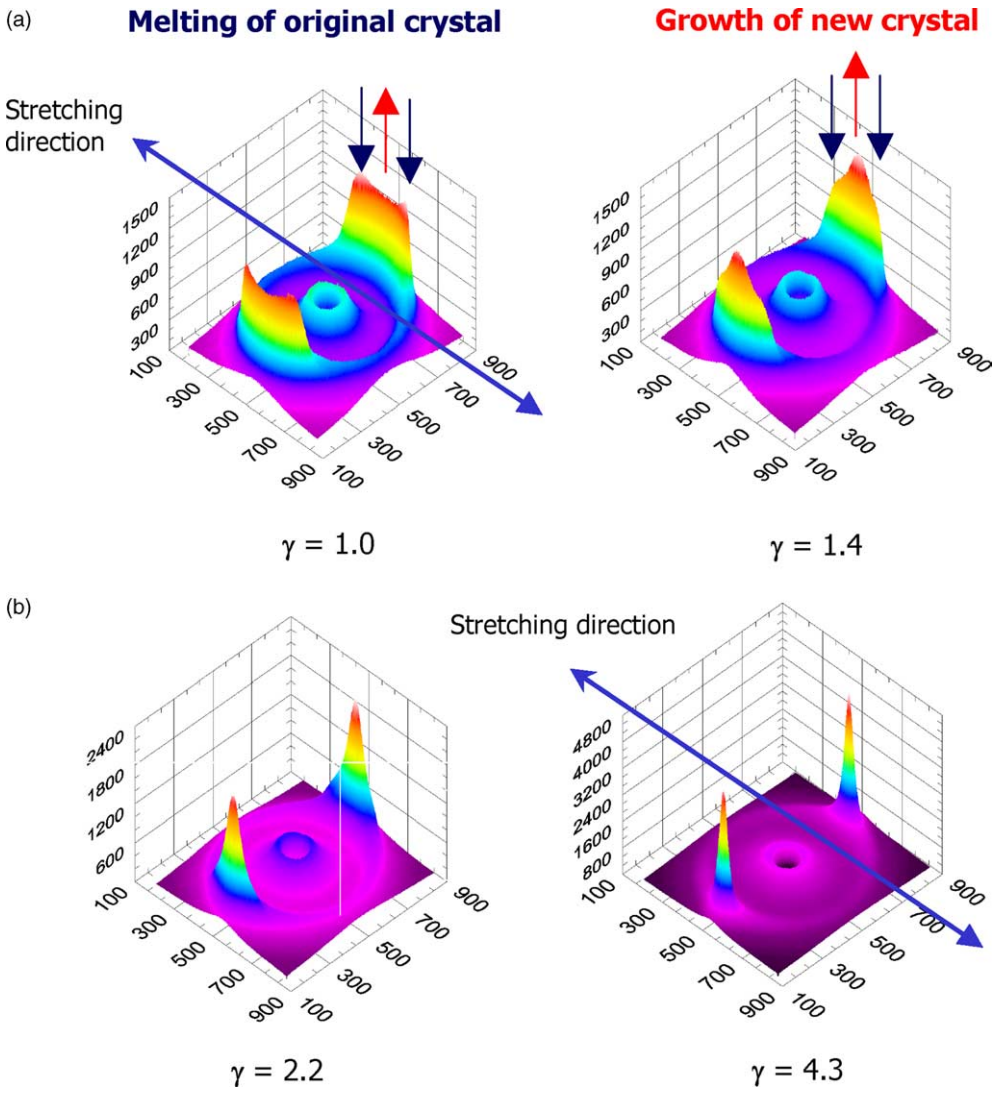

Fig. 8. 3D WAXD profiles of the EP copolymer at (a) strains of 1.0 and 1.4, and (b) strains of 2.2 and 4.3 (blue arrow indicates the diffraction from the initial crystals, and the red arrow indicates the diffraction from the new strain-induced crystals).

lamellae (e.g. those with their long axes along the stretching direction) is responsible for the four-arc scattering pattern seen in Fig. 7(b). Such composite morphology can also lead to the formation of the four-point pattern in WAXD (i.e. the splitting of the (100) reflection from the pseudo hexagonal form at the off-axes). SAXS and WAXD results provided complementary information. The SAXS data revealed the break-out and the orientation of the lamellar morphology [12], while the WAXD data provided the direct evidence of crystal destruction of selected crystalline lamellae and orientation of residual crystallites.

3.3. Deformation-induced re-crystallization at high strains

With the increase of strain from 0.5 to 1.0, the four-point (100) diffraction pattern gradually disappeared (Fig. 8(a)). Two features were observed: (1) a decrease in contribution from the original four-point pattern (we note that the azimuthal positions of the four peaks remained about constant) and (2) an increase in equatorial contribution from the newly developed pseudo hexagonal crystals. For example, at the strain of 1.4, the WAXD pattern became a two-bar pattern with the (100) reflection aggregated on the equator (Fig. 8(a)). The decreasing intensity in the four-point pattern indicated the crystal destruction of the original pseudo hexagonal crystals, while the increasing intensity in the two-bar equatorial pattern indicated the generation of new pseudo hexagonal crystals (i.e. strain-induced re-crystallization). The onset strain, at which new crystals began to grow, was found to be around 0.75, which was near the yield point. This finding was consistent with our earlier SAXS observations [12], which will be described briefly next. We hypothesize that the newly formed crystals are in the extended-chain conformation with its axes parallel to the stretching direction.

Our earlier SAXS study [12] indicated that when the strain reached 1.2, the newly developed crystal exhibited the same amount of scattering as the original crystals (this was evaluated by the integrated intensity from the 3-D SAXS profile). In addition, the scattering contribution from the original crystals totally disappeared at the strain of 1.5. The WAXD results in this work are consistent with the previous SAXS findings. For example, distinct equatorial (100) peaks from the strain-induced new crystals were seen at a strain of 2.2 (Fig. 8(b)). At strain 4.3, the (100) reflection was so sharp that the pattern became two-point like. It should be pointed out that at strains above 2.0, it is quite difficult to distinguish the scattering contributions between the amorphous segments and the new strain-induced crystal. This is because the scattering peak due to oriented amorphous segments at high strains somewhat overlapped the (100) diffraction peak from the strain-induced pseudo hexagonal crystals. This is seen in Fig. 9, where the linear WAXD intensity profiles taken along the equator at different strains (0.0–5.0) are shown. At high strains (>3.0), the amorphous background could not be easily separated from the crystal contribution. Thus, it is difficult to quantitatively evaluate the change in the crystallinity during the deformation process.

Fig. 10(a)–(c) shows 2D WAXD diffraction patterns taken at zero strain as well as at high strains (3.0 and 5.0) during the extension process. The sample-to-detection distance was adjusted so that higher order diffraction peaks (e.g. (110) and (200) reflections) could be detected. The oriented patterns at high strains are characteristic of the oriented pseudo hexagonal form, which has been reported before [3]. It should be noted that the oriented WAXD patterns were all from new crystals induced by deformation, rather than from original crystals before deformation. At strains above 5.0, the observed diffraction patterns (Fig. 10(c)) resembled that from the highly oriented fiber or single crystal, having excellent orientation along the stretching direction. The diffraction peaks can be indexed by the unit cell parameter $a=4.9$ Å of

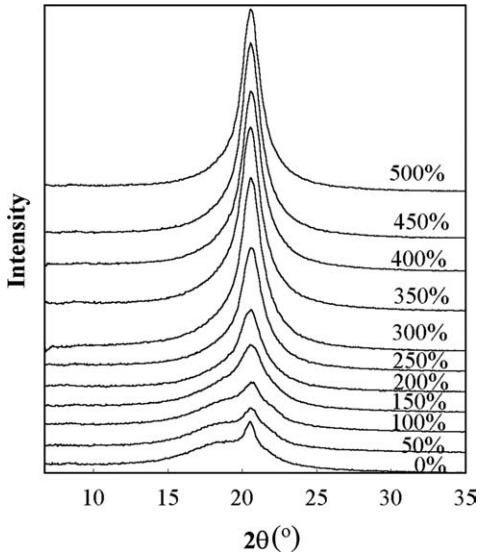

Fig. 9. Linear equatorial WAXD intensity profiles of the EP copolymer taken at different strains (from 0 to 5.0).

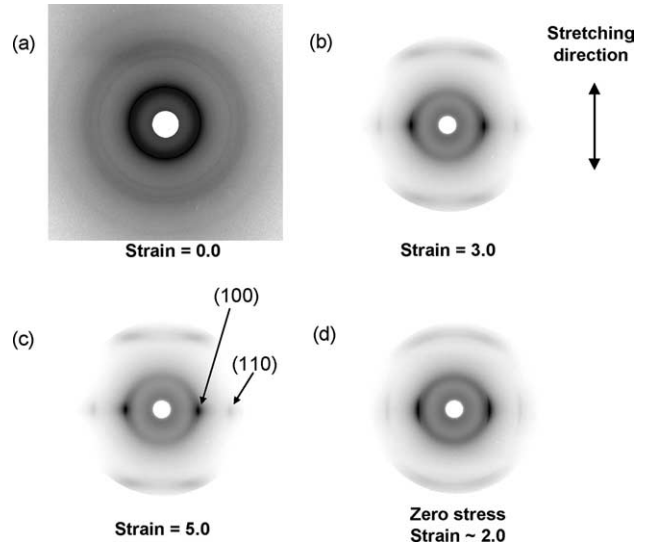

Fig. 10. WAXD patterns of the EP copolymer at strains of 0, 3.0, 5.0, and the pattern at zero stress after stretched sample relaxed to 200%.

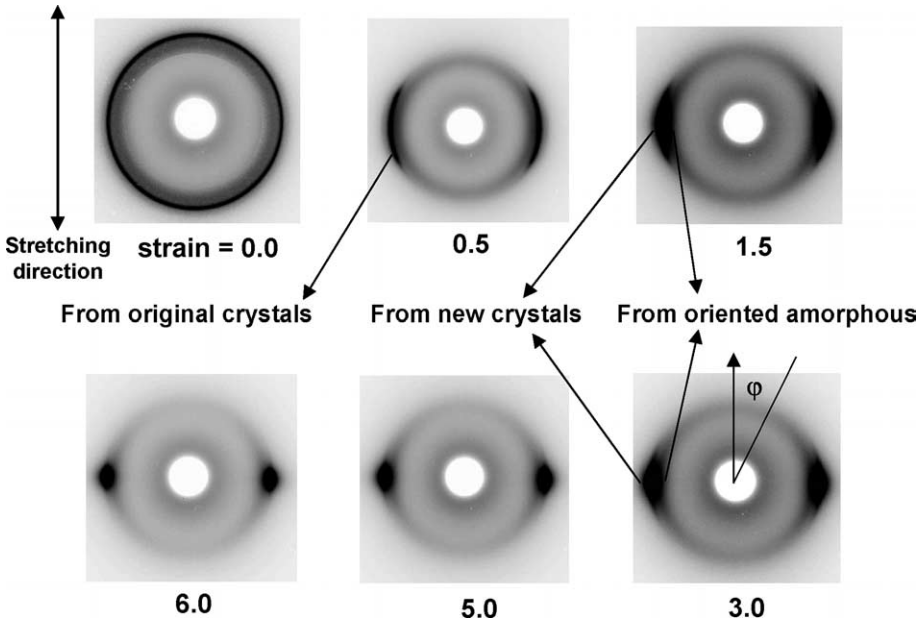

Fig. 11. WAXD patterns of the EP copolymer at strains of 0, 0.5, 1.5, 3, 5, and 6, respectively.

the pseudo hexagonal form as shown in Fig. 10(c). Both (100) and (110) reflections appeared on the equator, indicating that the chains in crystals were well aligned along the stretching direction, probably adopting an extended-chain conformation.

In our previous SAXS study [12], we found that when the load was completely relaxed during the retraction process, the strain-induced crystal lamellae remained largely intact and partially oriented along the stretching direction with a long period of 15 nm. Following the retraction process in Fig. 4, in situ WAXD patterns were also collected. Results indicated that both crystal orientation and crystal fraction (the exact amount could not be determined for the reasons described earlier, as well as in the discussion to follow) decreased with the reduction of strain. The WAXD pattern for the sample at zero load after being stretched to the strain of 6.0 is shown in Fig. 10(d), indicating that the crystal structure remained oriented with the pseudo hexagonal form, consistent with the SAXS results.

3.4. Orientation of amorphous phase under deformation

Under low deformation, strain-induced crystal destruction becomes more dominant (the original orthorhombic crystals appeared to be melted completely at strain 1.5) with the increase in strain; while under high deformation, strain-induced crystallization is the only dominant process. We hypothesize that the amorphous chains are stretched and oriented at high strains, which becomes precursor for strain-induced crystallization. The presence of the amorphous phase in the EP copolymer could be clearly identified in 2D WAXD patterns, since the amorphous phase appeared at a lower scattering angle than the crystal diffraction (e.g. the (100) reflection from the pseudo hexagonal form). The WAXD patterns, collected at a relatively long sample-to-detector distance to reveal the changes of the amorphous phase, are shown in Fig. 11. In this figure, the amorphous halo and the (100) diffraction ring were clearly separated at zero strain. At strain 0.5, both amorphous phase and the diffraction ring became oriented with their intensities aggregated around the equator (the (100) reflection was split into 4 arcs). At strain 1.5, the oriented amorphous phase could still be identified by the inner dark arcs near the equator. However, when the strain increased to 5.0, the equatorial diffraction from the (100) reflection and the equatorial scattering from the amorphous phase merged together, making it very difficult to differentiate the two.

In order to quantitatively evaluate the contribution of the oriented amorphous phase, diffraction profiles at different azimuthal angles (ϕ) with respect to the stretching direction were taken from the WAXD pattern at the strain of 3.0 (Fig. 11). These azimuthal profiles are shown in Fig. 12. The scattering profiles taken from $\phi = 0°$ (the stretching direction) to $\phi = 60°$ represented pure amorphous scattering, where the

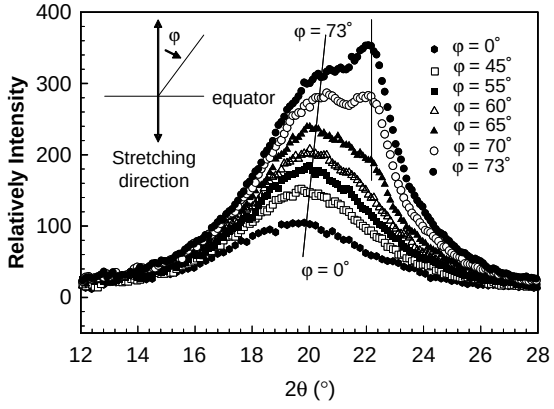

Fig. 12. Linear WAXD profiles taken along different azimuthal angles for the EP copolymer stretched at the strain of 3.0.

corresponding scattered intensity increased about 150%. The profile taken at $\phi = 65°$ showed a small diffraction contribution at $2\theta \sim 22°$, while this peak became distinct from the profile taken at $\phi = 70°$. It is interesting to note that the scattered intensity from the amorphous phase at $\phi = 73°$ increased about 200% over that taken along the stretching direction ($\phi = 0°$). In addition, the amorphous scattering peak was found to shift to a high diffraction angle with the increasing azimuthal angle. In fact, at the equator ($\phi = 90°$), the amorphous scattering peak and the (100) diffraction merged together (Fig. 9). These results indicated that a significant fraction of the amorphous chains in the deformed sample were aligned along the stretching direction. Similar analyses were also carried out on the patterns collected at strains above 3.0. It was found that the amorphous scattering peak near the equator was shifted to a higher 2θ angle with increasing strain, suggesting that the average interchain distance between the neighboring amorphous chains became smaller. We rationalize that the highly stretched and oriented EP amorphous chains with short interchain distance can promote the crystallization of ethylene sequences with extended-chain conformation, probably in a morphology assimilated to that of an oriented fringe-micelle, under high deformation.

4. Conclusions

In this study, several remarks can be concluded from in situ WAXD measurements of a semicrystalline EP copolymer containing 78 wt% of ethylene.

1. The crystalline structure of the chosen EP copolymer is a function of crystallization temperature. The high-crystallization temperature (e.g. 50 °C) favors the formation of the orthorhombic form, while the low-crystallization temperature (e.g. 20 °C) favors the formation of the pseudo hexagonal form.
2. At small stains (e.g. 0.12), the applied stress can transform the orthorhombic form to the pseudo hexagonal form in the chosen EP copolymer. The easy transformation is due to the very low-melting point of the crystals and the high mobility of the amorphous EP chains at room temperature.
3. At higher strains (≥ 0.25), WAXD results confirmed the processes of strain-induced crystal destruction (or mechanically-induced 'melting') and subsequent re-crystallization of the pseudo hexagonal form. The crystal destruction process of the pseudo hexagonal form probably takes place in lamellae aligned perpendicularly to the stretching direction through the chain pull-out mechanism. The resulting morphology, containing re-oriented (tilted) smaller fragmented lamellae and larger undamaged lamellae, is responsible for the four-arc patterns observed in both SAXS and WAXD images.
4. Detailed WAXD analysis showed that the degree of orientation of the amorphous chains increased rapidly with increasing strain. The highly stretched and oriented amorphous chains appear to be the precursors of strain-induced crystallization at high strains.

Acknowledgements

This work was supported by an NSF grant (DMR-0405432). The WAXD synchrotron beamline X27C was supported by the Department of Energy (Grant DE-FG02-99ER 45760).

References

[1] Albizzati E, Giannini U, Collina G, Noristi L, Resconi L. In: Moore Jr EP, editor. Polypropylene handbook. New York: Hanser Publishers; 1996. p. 419.
[2] Bassi IW, Corradini P, Fagherazzi G, Valvassori A. Eur Polym J 1970;6:709.
[3] de Ballesteros OR, Auriemma F, Guerra G, Corradini P. Macromolecules 1996;29:7141.
[4] Guerra G, de Ballesteros OR, Venditto V, Galimberti M, Sartori F, Pucciarello R. J Polym Sci, Part B: Polym Phys 1999;37:1095.
[5] Kolbert AC, Didier JG, Xu L. Macromolecules 1996;29:8591.
[6] Mathot VBF, Scherrenberg RL, Pijipers MFJ, Bras J. Therm Anal 1996;46:681.
[7] Minick J, Moet A, Hiltner A, Baer E, Chum P. J Appl Polym Sci 1995;58:1371.
[8] Ran S, Zong X, Fang D, Hsiao BS, Chu B. J Appl Crystallogr 2000;33:1031.
[9] Ran S, Zong X, Fang D, Hsiao BS, Chu B, Phillips RA. Macromolecules 2001;34:2569.
[10] Ran S, Burger C, Fang D, Zong X, Cruz S, Hsiao BS, et al. Macromolecules 2002;35:433.
[11] Somani RH, Hsiao BS, Nogales A, Srinivas S, Tsou AH, Sics I, et al. Macromolecules 2000;33:9385.
[12] Liu L, Hsiao BS, Fu BX, Ran S, Toki S, Chu B, et al. Macromolecules 2003;36:1920.
[13] Ran S, Wang Z, Burger C, Chu B, Hsiao BS. Macromolecules 2002;35:10102.
[14] Tashiro K, Sasaki S, Kobayashi M. Macromolecules 1996;29:7460.
[15] Uehara H, Kanamoto T, Kawaguchi A, Murakami S. Macromolecules 1996;29:1540.
[16] Hu W, Srinivas S, Sirota B. Macromolecules 2002;35:5013.
[17] Warren BE. X-ray diffraction. New York: Dover Publications; 1990.
[18] Fraser RDB, Marae TP, Miller A, Rowlands RJ. J Appl Crystallogr 1976;9:81.